

TEMPO-Oxidized Cellulose Hydrogel Fiber Cell Load, a Cell Support System Proof of Concept

Mariana Alves Rios

University of Araraquara: Universidade de Araraquara

Paula About Barbugli

UNESP: Universidade Estadual Paulista Julio de Mesquita Filho

Mônica Rosas Costa lemma

University of Araraquara: Universidade de Araraquara

Rafael Grande

Aalto University Department of Bioproducts and Biosystems

Antônio José Felix Carvalho

USP: Universidade de Sao Paulo

Eliane Trovatti (✉ elianetrov@yahoo.com.br)

University of Araraquara: Universidade de Araraquara <https://orcid.org/0000-0002-0495-8115>

Research Article

Keywords: osteo-1 cells, TEMPO, cellulose nanofiber hydrogel, complexation, fiber

Posted Date: April 13th, 2021

DOI: <https://doi.org/10.21203/rs.3.rs-368033/v1>

License:   This work is licensed under a Creative Commons Attribution 4.0 International License.

[Read Full License](#)

Abstract

The development of new cell carriers systems are crucial for application in regenerative medicine, once they deliver the cells to the injured tissue to trigger the repair and stimulate the regeneration of the new tissue, and so far various carrier systems have been investigated in this regard. Here we report on the synthesis and characterization of a new cell carrier system in fiber shape where the cells osteo-1 are incorporated into the oxidized cellulose nanofibers suspension and then complexed with calcium ions in a pulling process giving rise to the fiber loaded with cells. The microscopic images showed the success of the proposed method to incorporate the cells into the fibers. The results of the in-vitro viability tests indicated the capability of the fibers to keep the cells alive and to mineralize them, indicating that their osteogenic capability was not affected. In addition, the fiber disintegration studies showed the system is capable of releasing the cells, suggesting the potential of the fibers as a new assembled hydrogel carrier cell therapy.

1. Introduction

Hydrogels based on biopolymers, are promising materials for use in regenerative medicine because of their properties such as biocompatibility and high water content, which allows oxygen and nutrients to permeate it, providing the adequate environment for cells signaling, proliferation (Hospodiuk et al. 2016) and improving the interaction with cells (Triplett and Budinskaya, 2017). The conventional cells administration, normally carried out in liquids injectable vehicles, can lead to the local cell aggregation, migration or distribution to undesired tissues, decreasing the cell survival at the local of the lesion, decreasing also the efficiency of the treatments (Herberts et al. 2011), mainly because the lack of an appropriate vehicle to accommodate and keep the cells at the site of the administration. The cross-linked hydrogels can keep the tridimensional structure, without dissolution, supporting and mimicking the cells natural environment before disintegration. In cell therapy, the maintenance of the cells at the site of the injury favors the new tissue formation, increases the speed of the repair and the reconstruction of the pristine tissue. New materials for cell delivery based on viscous solutions of natural polymers have been widely studied (Triplett and Budinskaya, 2017), however, few non covalent cross-linked examples are described in the literature, and the most studied are the calcium alginate (Draged et al. 1997; Draged et al. 1998) based systems.

Nanofibrillated cellulose (CNF)- based hydrogels have been investigated as a promising nanostructured biomedical material owing its biocompatibility and absence of human cytotoxicity (Aljohani et al. 2017; Jorfi and Foster, 2015; Klemm et al. 2005; Salimi et al, 2019). The oxidation of CNF hydroxyls to carboxyl groups using 2,2,6,6-tetramethylpiperidine-1-oxyl (TEMPO catalyst) is one of the most used methods to introduce negative charges on cellulose fibers which increases cellulose hydrophilicity (Saito et al. 2006) and giving rise to concentration-dependent viscosity hydrogel formed by individualized nanofibrils (Saito et al. 2006) (Singh et al. 1982) (Weishaupt et al. 2015). Carboxylate groups are also appropriate to crosslink cellulose by ionic complexation (Carvalho et al. 2016) (Grande et al. 2017), which may be used as a bottom-up approach to obtain flexible scaffolds with superior cell distribution. TEMPO oxidized

cellulose nanofibers (ToCNF) derivative can be assembled into beads with 0.5–3 mm diameter (Carvalho et al., 2016) or fibers with 0.2 mm diameter (Grande et al., 2017) by ionic complexation. Several tissues are naturally organized in fiber shape, including the nervous system and the striated muscle, the most challenging tissues to be repaired. Fibers loaded with cells can be used to guide the regeneration of these noble tissues, mimicking their pristine arrangement. However, engineering a complex 3D construct for in situ cell encapsulation in a bulk hydrogel is challenging and few systems comprising fiber cell loading and delivery structures have been reported. (Laurén et al. 2017; Kalisky et al. 2016). In this vein, here we propose to prepare ToCNF fibers loaded with cells aimed at harnessing the versatility of these fibers towards potential applications that involve cell loading/release for regenerative medicine application.

For such, the cells are incorporated into the ToCNF suspension, a drop of the cell loaded suspension was put in contact with a drop of calcium chloride solution and pulled out for the fiber formation. To the best of our knowledge, the preparation of fibers from ToCNF and CaCl_2 and its loading with cells is described here for the first time. The presence of cells within the fibers was analyzed by optical microscopy and their viability by resazurin and mineralization studies. The proposed fiber-based cell carrier system represents a promising material, once they can burst the technology in such a field.

2. Results And Discussion

2.1. ToCNF preparation and characterization

Figure 1 top panel depicts sugarcane bagasse conversion in nanofibrilated cellulose suspension and at bottom panel, FTIR spectra of CNF and ToCNF, the conductometric titration curve of ToCNF and SEM image of ToCNF. Figure 1A shows sugarcane bagasse after Soxhlet extraction, in which the fibers agglomerate are large (~ 1 mm length) and brownish due to the presence of lignin (Fig. 1A), Fig. 1B and C shows the bleached sugarcane bagasse after lignin extraction prior oxidation and after oxidation, respectively. Figure 1D shows the sonicated transparent aqueous ToCNF gel, and its respective scanning electron microscopy image (Fig. 1E). The CNF suspension (Fig. 1C) is formed by the agglomerated CNF, visible at naked eye. The nanofibers separation by mechanical deconstruction using the ultrasonication processes generated the high viscous transparent gel (Fig. 1D). CNF and ToCNF FTIR spectra (Fig. 1F) displayed typical absorption bands of cellulosic substrates at 3300, 2880 and 1100 cm^{-1} , corresponding to the vibrations of the O-H, C-H and C-O groups of cellulose, respectively. ToCNF spectra displays, in addition to the typical cellulose bands, a strong band at 1600 cm^{-1} , which correspond to the vibrations of the carboxylic group, indicating the success of the oxidation reaction, in agreement with the literature (Saito et al. 2007). Conductometric titration (Fig. 1G) was used to determine the content of carboxylic groups formed by the oxidation reaction, which resulted in 1.8 mmols.g⁻¹ of ToCNF, confirming the success of the reaction.

2.2. ToCNF fibers preparation and cell loading

The preparation of the cell loaded fibers followed the principle previously described in our research group (Grande et al. 2017), in which the fiber is generated by ionic complexation of anionic ToCNF with a cationic polymer macromolecule. Cell loading was carried out by centrifuging growth cells and then, dispersing cells pellet into the ToCNF suspension prior the fiber spinning. The fiber drawing method consisted in depositing a droplet of the ToCNF suspension loaded with cells and a droplet of CaCl_2 solution onto a Petri dish and joining the drops using the tweezers in such a way that the two drops were in lateral contact. The interface of the drops and gently pulled by using tweezers, giving rise to the cell loaded fiber, as schematized in Fig. 2. The fiber was pulled out from the interface formed by the positive and the negative charged components.

Figure 3 depicts the fiber formation process. Droplets from CaCl_2 solution and ToCNF/cell suspension were deposited on the Petri dish (A). Upon the droplets contact, a viscous interface is generated by interfacial ionic complexation (B, C). Dragging the viscous interface upwards (D), leads to the formation of the long hydrogel fiber (E). The still wet fiber is immersed in the culture medium.

The formation of the crosslinked gel was capable of supporting the dispersed cells within the fibers. The tridimensional network environment was formed by the interaction of two negatively charged group on ToCNF surface (from one or two fibers) with one divalent calcium ion, generating the cross linking and leading the fiber to assembly when pulled. The presence of the cells in ToCNF suspension allow them to be loaded and accommodated into the born gel fibers. The dispersion of the cells within the fibers can be the result of these strong electrostatic forces which cross link ToCNF with the calcium ions. Thus, even the large cell size (about 50 μm) when compared to the ToCNF nanofibers ($\sim 20 \text{ nm}$), they remain dispersed because of the mechanically stable tridimensional network hydrogel.

2.3. Cell viability

The results of viability measurements, the images of the cell within the fibers and their nuclei marked with the fluorescent DNA marker DAPI, are shown in Fig. 4. The cells' distribution within the fibers were followed by bright field optical microscopy and confocal fluorescence microscopy. The optical microscopy of the fiber free of cells, Fig. 4A, shows the appearance of a transparent fiber. Figure 4B shows the fiber loaded with cells, in which several cells are seen as dark points homogeneous distributed along the fibers. The confocal microscopy (Fig. 4C, D and E) shows the images of the fluorescent cells nuclei marked with DAPI. The results clearly indicated the tridimensional distribution of the cells within the fibers, in which, the depth reached by the technique was about 300 μm from the fiber surface. These results indicated the tridimensional distribution of the cells within the fibers, as shown by the cross section in Fig. 4G, H and I. The image showed in Fig. 4E reveal a higher density of cells into the fiber from 48 h of incubation, suggesting the cell proliferation. The cell viability (Fig. 4F) was determined using the resazurin method. In this method, the resazurin is inserted into the culture media and its metabolism by living cells generate the fluorescent product resorufin, which is used to estimate the cell viability. The fluorescence intensity is proportional to the number of alive cells (cell viability). The results suggested a tendency to increase, however, with no significant differences for the values at zero and 24 h, and with no

significant difference when comparing the 24 and 48 h viability values, indicating the cells kept alive during all the measured incubation time.

One of the most important properties of the materials for cell delivery is the maintenance of the cell viability. For such, the permeability of the small molecules such as oxygen and carbohydrates are crucial for the cell's survival. The cell viability within the fibers indicated the ToCNF fibers were permeable to oxygen and nutrients, keeping the cells alive for all the period of the experiment, 48 h. The results indicated the success of the fiber cell loading method and the capability of the fibers shape and composition to keep the cells alive within it.

2.4. Osteogenic potential of the cells after loading into the fibers

The osteogenic potential experiment was carried out to evaluate if the cells kept their differentiation capability after being loaded and kept within the fibers, as an indicative of their healthiness. Calcium deposition on the extracellular matrix indicates the late osteogenesis as the result of the osteoblasts precursors cells maturation (Smieszek et al. 2020) and can be used to evaluate if the cells kept their capability of differentiation. The principle of the method is based on the complexation reaction in which one mole of Alizarin red binds to two moles of calcium forming the dark red Alizarin red-calcium complex. Figure 5A shows the result of the cells maintained for 15 days under osteogenic conditions and marked with Alizarin red. The dark red calcium deposits (some of them indicated by arrows) is the result of the Alizarin Red-calcium complex formation and precipitation, indicating that the mineralized matrix was formed and that cells properly differentiate. The result indicated that the cells kept its property of differentiation, once the mineral matrix was formed, even loaded within the fibers. Figure 5B shows the result of the fiber free of cells marked with alizarin red, in which no calcium deposits could be seen. This fiber was used as the control, once calcium ions were used to drawing the fibers, and the results indicated it does not lead to the formation of calcium deposits.

2.5. Fiber disintegration

The disintegration study was carried out in order to evaluate the capability of the fibers to release the cells. For such, the fibers were inserted into the wells of the microplate filled with phosphate buffer saline (PBS). The PBS exchanging simulated the body fluids circulation, leaching the local salts. The repeated leaching is capable of removing or exchanging the salts from the poly-ion complex formed by calcium salts and ToCNF, leading the fiber to slowly degrade. It can be seen as a positive property of the fibers, once the cells can be released when it disintegrates. Figure 6 shows the image of the whole fiber (A), the starting disintegration step (B) and the advanced disintegration step (C). At the second and third steps some dark agglomerates were observed in all the fibers and could be attributed to the small agglomerates of fibers released during the disintegration.

The hydrogel fibers could be used in clinical approaches as cell carriers for releasing these cells at the injured site, in which they will proliferate and differentiate for repair the damaged tissue. The capability of the fibers to keep the cells alive without losing their intrinsic capabilities, such as the differentiation, and its slow disintegration, releasing the cells in a controlled period of time indicate the potential of the material for use in cell therapy in regenerative medicine. The hydrogel fibers display large diameter (1–2 mm, Fig. 4C), interesting features for guiding the regeneration in an organized arrangement of cells after the degradation of the ToCNF matrix, they can also be used for filling critical lesions and as a matrix (bioink) for bioprinting applications.

3. Conclusions

The preparation of TEMPO oxidized cellulose nanofibers fibers and its loading with cells aiming to develop a novel cell carrier system is reported here for the first time. The fibers were prepared by ionic complexation of complexation of TEMPO oxidized cellulose nanofibers and calcium ions in a drawing process, in which the cells were incorporated into the ToCNF suspension. The cells incorporation into the fibers were shown by bright field optical microscopy and confocal fluorescence microscopy. The capability of the fiber to keep the cells alive was demonstrated by viability studies and its release capability was shown by the degradation of the fibers in PBS after 3–7 days of incubation. The deposition of the extracellular mineralized matrix indicated that the cells differentiation capability was not affected by incorporation into the fibers. The results showed the proof of concept of incorporating and keeping the cells alive within the fibers represent a promising strategy for application in cell therapy, mainly as a scaffold for guiding the repair of tissues in which the cells grow in fibrillar shape, or for reconstitution of layer by layer tissue with different cell types. The material can also be useful for bioprinting and regenerative medicine in general.

Declarations

Funding

This work was supported by the São Paulo Research Foundation (FAPESP) under Grant 2017/18782-6 (E.T.) and 2018/06555-8 (M.A.R.) and National Council for Scientific and Technological Development (CNPq) under Grant 307124/2015-0 and 303847/2019-0 (A.J.F. C.).

5. COMPLIANCE WITH ETHICAL STANDARDS

Statement of research involving Human Participants and/or Animals

The research did not involve human participants.

The research did not involve animals.

Conflict of interest

There are no conflict of interest to declare.

References

1. Brodin FW, Gregersen, ØW, Syverud K (2018). Cellulose nanofibrils: Challenges and possibilities as a paper additive or coating material – A review. *Nordic Pulp & Paper Research Journal*, 29: 156–166 <https://doi.org/10.3183/npprj-2014-29-01-p156-166>
2. Carvalho RA, Veronese G, Carvalho AJF, Barbu E, Amaral AC, Trovatti E (2016) The potential of TEMPO-oxidized nanofibrillar cellulose beads for cell delivery applications. *Cellulose*, Springer Science, 23: 3399–3405. <https://doi.org/10.1007/s10570-016-1063-2>
3. Draget KI, Skjåk-Bræk, G, Smidsrød O (1997) Alginate based new materials. *International Journal of Biological Macromolecules*, 21: 47–55. [https://doi.org/10.1016/S0141-8130\(97\)00040-8](https://doi.org/10.1016/S0141-8130(97)00040-8)
4. Draget KI, Steinsvåg K, Onsøyen E, Smidsrød O (1998) Na- and K-alginate; effect on Ca²⁺-gelation. *Carbohydrate Polymers*, 35: 1–6. [https://doi.org/10.1016/S0144-8617\(97\)00237-3](https://doi.org/10.1016/S0144-8617(97)00237-3)
5. Grande R, Trovatti E, Carvalho AJF, Gandini A (2017) Continuous microfiber drawing by interfacial charge complexation between anionic cellulose nanofibers and cationic chitosan. *Journal of Materials Chemistry A*, 5: 13098–13103. <https://doi.org/10.1039/C7TA02467C>
6. Herberts CA, Kwa MS, Hermsen HP, (2011) Risk factors in the development of stem cell therapy. *Journal of Translational Medicine*, 9:29 <https://doi.org/10.1186/1479-5876-9-29>
7. Homma I, Fukuzumi H, Saito T, Isogai A (2013) Effects of carboxyl-group counter-ions on biodegradation behaviors of TEMPO-oxidized cellulose fibers and nanofibril films. *Cellulose*, 20: 2505–2515. <https://doi.org/10.1007/s10570-013-0020-6>
8. Hospodiuk M, Dey M, Sosnoski D, Ozbolat IT (2016) The bioink: A comprehensive review on bioprintable materials. *Biotechnology Advances* 35: 217–239. <https://doi.org/10.1016/j.biotechadv.2016.12.006>
9. Isogai A, Saito T, Fukuzumi H, (2011) TEMPO-oxidized cellulose nanofibers. *Nanoscale* 3: 71–85 <https://doi.org/10.1039/C0NR00583E>
10. Jorfi M, Foster J (2015) Recent advances in nanocellulose for biomedical applications. *Journal of Applied Polymer Science* 132: 41719. <https://doi.org/10.1002/app.41719>
11. Kalisky J, Raso J, Rigother C, Rémy M, Siadous R, Bareille R, Fricain JC, Amedée-Vilamitjana J, Oliveira H, Devillard R (2016) An easy-to-use and versatile method for building cell-laden microfibres. *Scientific Reports*, 6:33328. <https://doi.org/10.1038/srep33328>
12. Klemm, D, Heublein, B, Fink, HP, Bohn A (2005) Cellulose: Fascinating biopolymer and sustainable raw material. *Angewandte Chemie International* 44: 3358–3393. <https://doi.org/10.1002/anie.200460587>
13. Laurén P, Somersalo P, Pitkänen I, Lou Y-R, Urtti A, Partanen J, Seppälä J, Madetoja M, Laaksonen T, Mäkitie A, Yliperttula M (2017) Nanofibrillar cellulose-alginate hydrogel coated surgical sutures as cell-carrier systems. *PLoS ONE*, 12: e0183487. <https://doi.org/10.1371/journal.pone.0183487>

14. Saito T, Kimura S, Nishiyama Y, Isogai A (2007) Cellulose Nanofibers Prepared by TEMPO-Mediated Oxidation of Native Cellulose. *Biomacromolecules* 8: 2485 – 249. <https://doi.org/10.1021/bm0703970>
15. Saito T, Nishiyama Y, Putaux J L, Vignon M, Isogai A (2006) Homogeneous Suspensions of Individualized Microfibrils from TEMPO-Catalyzed Oxidation of Native Cellulose. *Biomacromolecules*, 7: 1687–1691. <https://doi.org/10.1021/bm060154s>
16. Salimi S, Sotudeh-Gharebagh R, Zarghami R, Chan SY, Yuen KH (2019) Production of nanocellulose and its applications in drug delivery: A critical review. *ACS Sustainable Chem* 7: 15800–15827. <https://doi.org/10.1021/acssuschemeng.9b02744>
17. Singh M, Ray AR, Vasudevan P (1982) Biodegradation studies on periodate oxidized cellulose. *Biomaterials*, 3: 16–20. [https://doi.org/10.1016/0142-9612\(82\)90055-2](https://doi.org/10.1016/0142-9612(82)90055-2)
18. Smieszek A, Marcinkowska K, Pielok A, Sikora M, Valihrach L, Marycz K (2020) The Role of miR-21 in Osteoblasts–Osteoclasts Coupling In Vitro. *Cells*, 9: 479. <https://doi.org/10.3390/cells9020479>
19. Triplett RG, Budinskaya O (2017) New Frontiers in Biomaterials. *Oral and Maxillofacial Surgery Clinics* 29:105–115. <https://doi.org/10.1016/j.coms.2016.08.011>
20. Weishaupt R, Siqueira G, Schubert M, Tingaut P, Maniura-Weber K, Zimmermann T, Ihssen J (2015) TEMPO-oxidized nanofibrillated cellulose as a high density carrier for bioactive molecules. *Biomacromolecules*, 16: 3640–3650. <https://doi.org/10.1021/acs.biomac.5b01100>

Figures

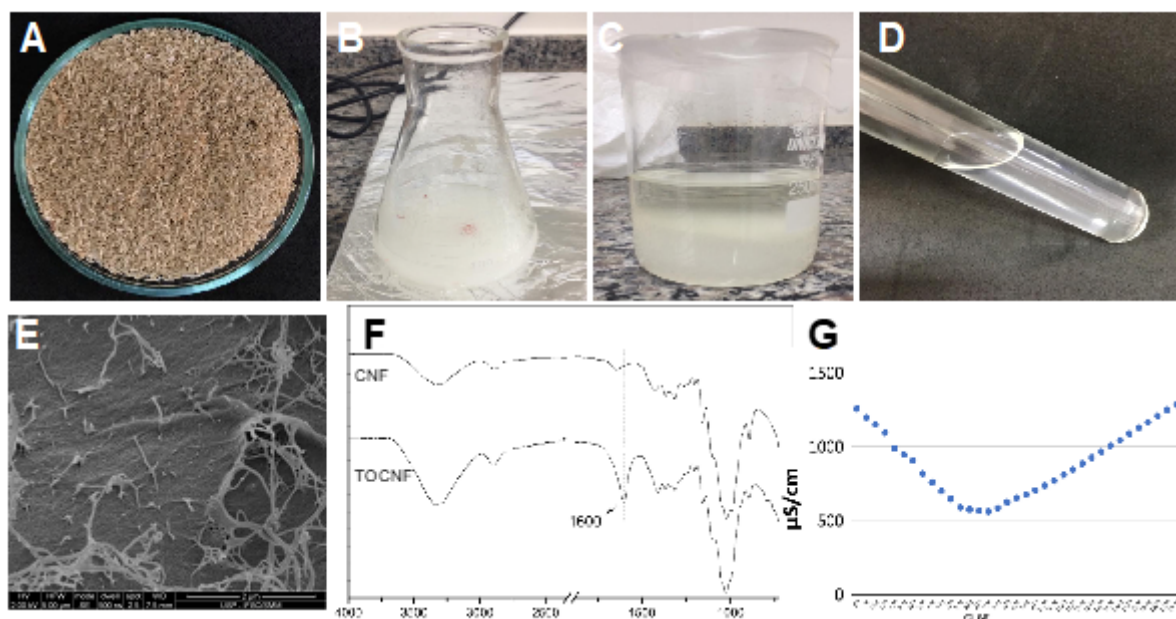


Figure 1

(A) Raw sugarcane bagasse, (B) CNF suspension, (C) ToCNF suspension before homogenization, (D) homogenized ToCNF suspension, (E) SEM of ToCNF, (F) FTIR spectra of CNF and ToCNF, (G)

Conductometric titration curve of ToCNF.

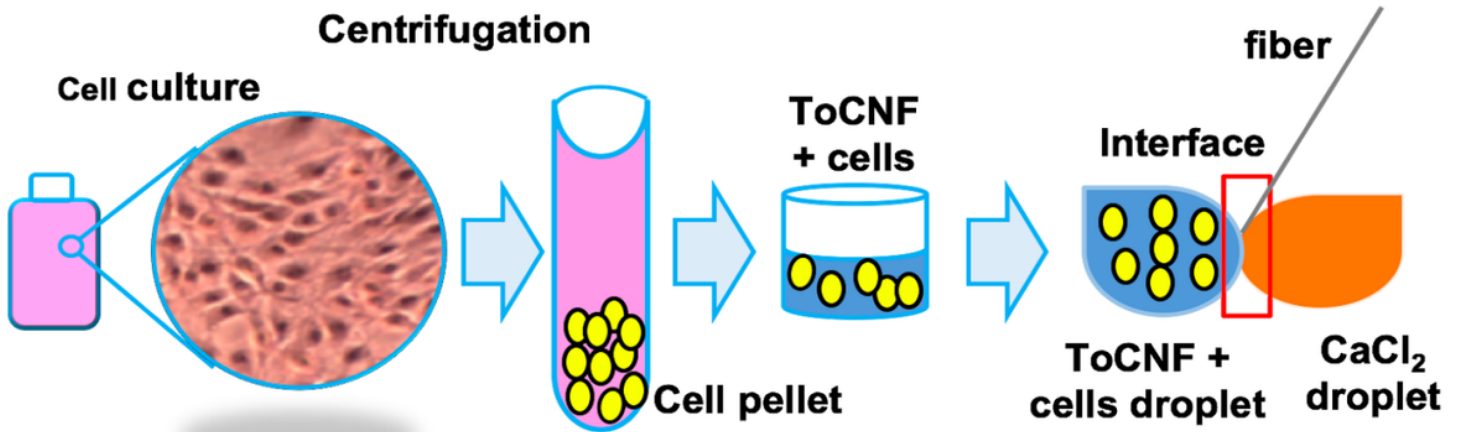


Figure 2

Scheme of the preparation of the cell loaded ToCNF fiber

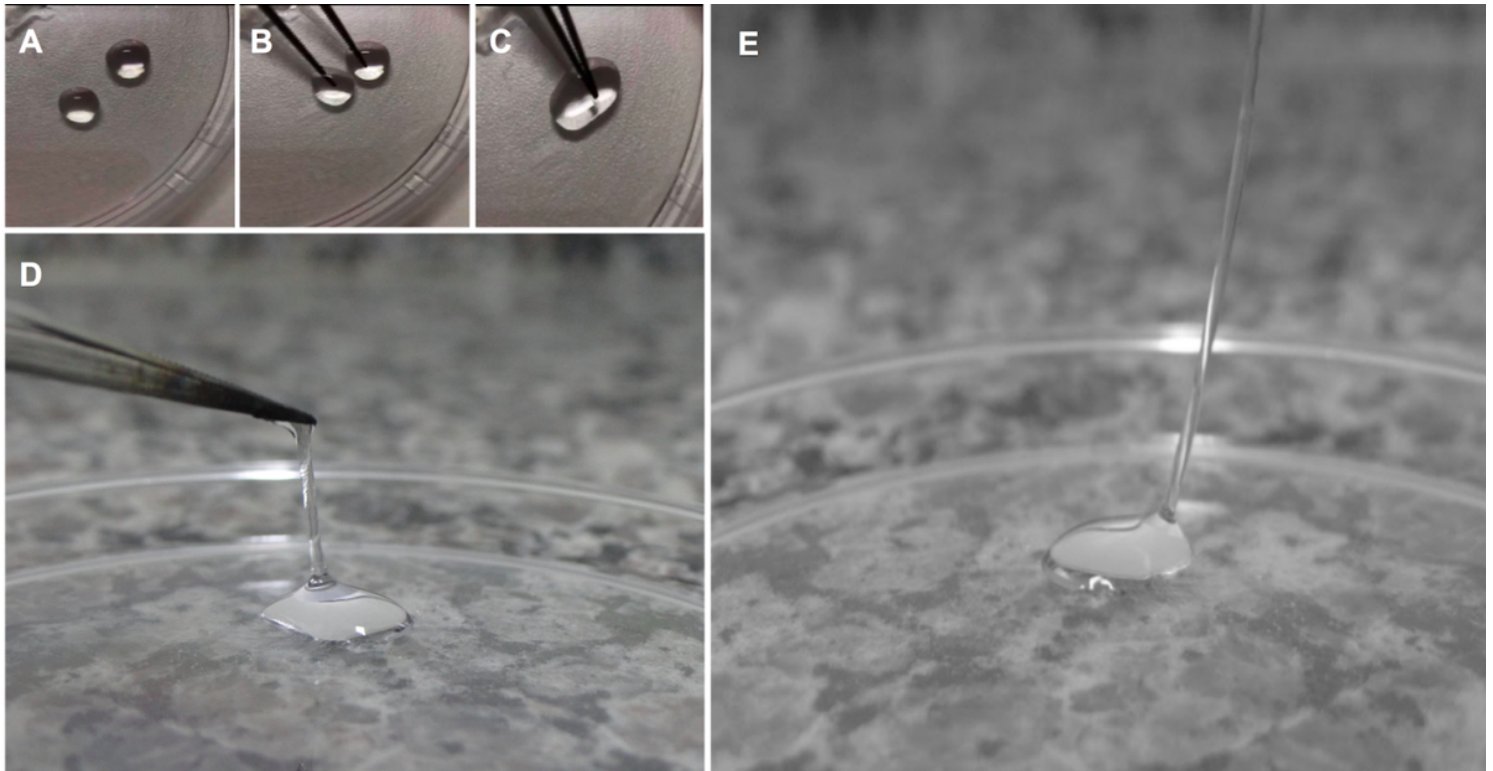


Figure 3

The droplets of CaCl₂ and ToNF on the Petri dish (A), their approximation with the tweezers (B), the tweezers into the interface (C) and the fiber hydrogel (D and E).

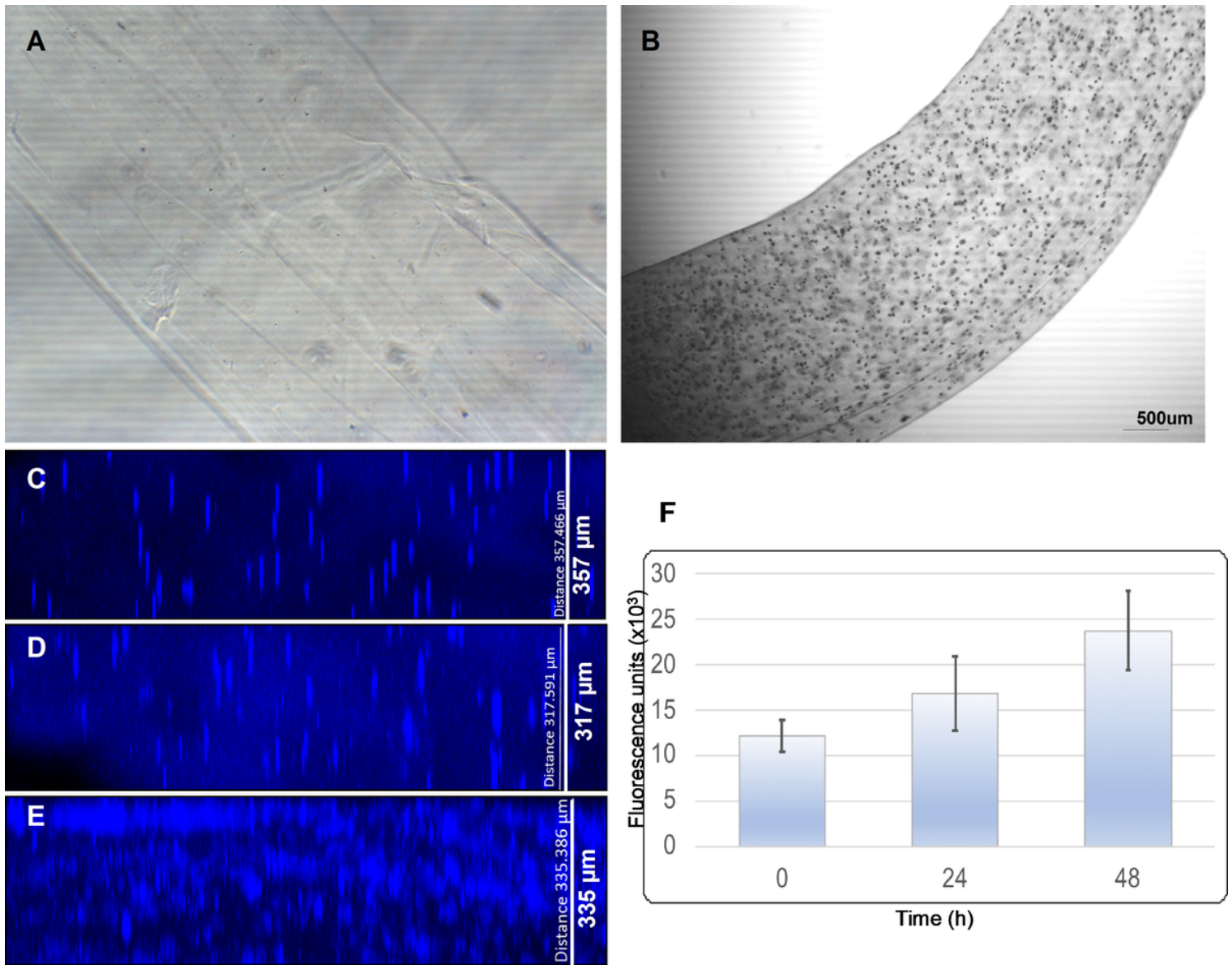


Figure 4

The images of optical microscopy of the fiber free of cells (A) and loaded with cells (B), the confocal microscopy at 0, (C) 24 (D) and 48 h (E) of incubation, showing the fluorescent cells nuclei marked with DAPI and the results of viability measurements (F).

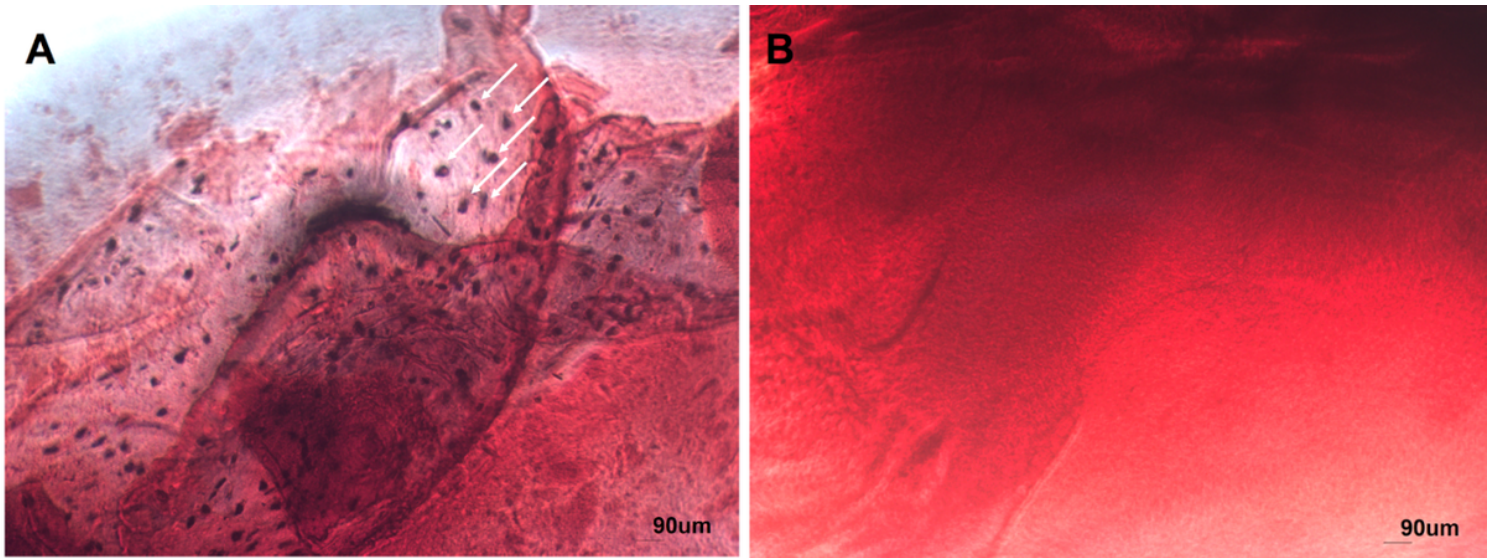


Figure 5

Alizarin red staining showing the calcified dark red nodules deposition after 14 days in culture.

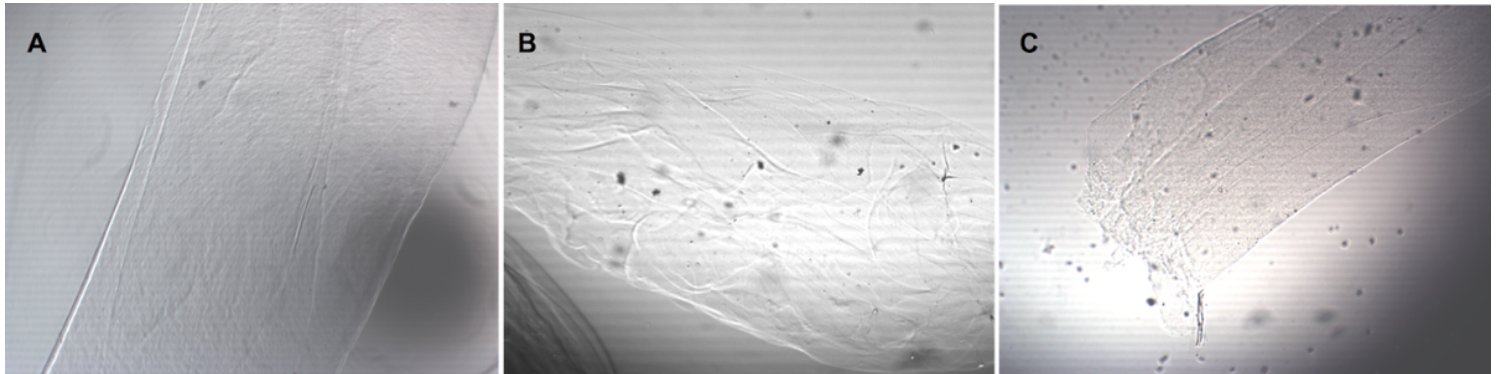


Figure 6

Fiber disintegration in PBS at zero (A), 3rd (B) and 7th (C) days time points.

Supplementary Files

This is a list of supplementary files associated with this preprint. Click to download.

- [WhatsAppVideo20201206at20.35.10.mp4](#)
- [supplemmat2.docx](#)